Official Journal of CIOMP
elight.springeropen.com

RESEARCH ARTICLE

Open Access

High-frequency terahertz waves disrupt Alzheimer's β-amyloid fibril formation

Wenyu Peng[1,2], Zhi Zhu[3*], Jing Lou[2], Kun Chen[4], Yuanming Wu[1*] and Chao Chang[2,5*]

Abstract

The accumulation and deposition of amyloid can cause a variety of neurodegenerative diseases, including Alzheimer's and Parkinson's disease. The degradation or clearance of this accumulation is currently the most widely accepted therapeutic strategy for intervention in these pathologies. Our study on amyloid-β (Aβ) oligomers in vitro revealed that high-frequency terahertz (THz) waves at a specific frequency of 34.88 THz could serve as a physical, efficient, non-thermal denaturation technique to delay the fibrotic process by 80%, as monitored by a thioflavine T (ThT) binding assay and Fourier transform infrared (FTIR) spectroscopy. Additionally, THz waves of this frequency have been shown to have no side effects on normal cells, as confirmed by cell viability and mitochondrial membrane potential assays. Furthermore, molecular dynamic (MD) simulations revealed that the THz waves could resonate with Aβ fibrils, disrupting the dense conformation by breaking the β-sheet structure and promoting the formation of abundant coil and bend structures. This study uses the amyloid of Aβ as an example, and the results will further guide interventions for the accumulation of other amyloids, which may provide new ideas for the remission of related diseases.

1 Introduction

Amyloid deposition is a hallmark of neurodegenerative diseases such as Alzheimer's disease (AD) and Parkinson's disease (PD) and the most prominent amyloid proteins include β-amyloid (Aβ), tau and α-synuclein [1, 2]. In vitro, the deposition process has been described as a sigmoidal curve in which misfolded proteins assemble into oligomers prior to fibril elongation and finally reach a plateau [3]. This dynamic process is accompanied by misfolded monomers with more α-helical structure forming abundant crosslinked β-sheet structures, resulting in neurotoxicity [4, 5]. Thus, targeting toxic accumulation may represent a promising strategy to slow or prevent disease initiation [6–8]. In this research, we used amyloid β (Aβ) as an example to conduct the research, which does not indicate that Aβ plays a determining role in AD development. Increasing research has also begun to emphasize the significance of tau protein [9–11] (Fig. 1). Fortunately, amyloid proteins have similar dynamic aggregation processes [4]. Although many studies have been based on small molecules, there are still no effective drugs that can inhibit or alleviate the deterioration of AD pathology [9, 12]. The present study intends to regulate the conformations of pathological proteins by optical techniques that intervene the dynamic process. This research that based on Aβ may be further applied to tau protein, which is of great significance for the development of combination therapy.

*Correspondence:
Zhi Zhu
zhuzhi@usst.edu.cn
Yuanming Wu
wuym@fmmu.edu.cn
Chao Chang
gwyzlzssb@pku.edu.cn
[1] Department of Biochemistry and Molecular Biology, Shaanxi Provincial Key Laboratory of Clinic Genetics, School of Basic Medicine, Air Force Medical University, Xi'an 710032, China
[2] Innovation Laboratory of Terahertz Biophysics, National Innovation Institute of Defense Technology, Beijing 100071, China
[3] Key Laboratory of Optical Technology and Instrument for Medicine, Ministry of Education, College of Optical-Electrical and Computer Engineering, University of Shanghai for Science and Technology, Shanghai 200093, China
[4] Department of Anatomy, Histology and Embryology and K.K. Leung Brain Research Centre, School of Basic Medicine, Air Force Medical University, Xi'an 710032, China
[5] School of Physics, Peking University, Beijing 100871, China

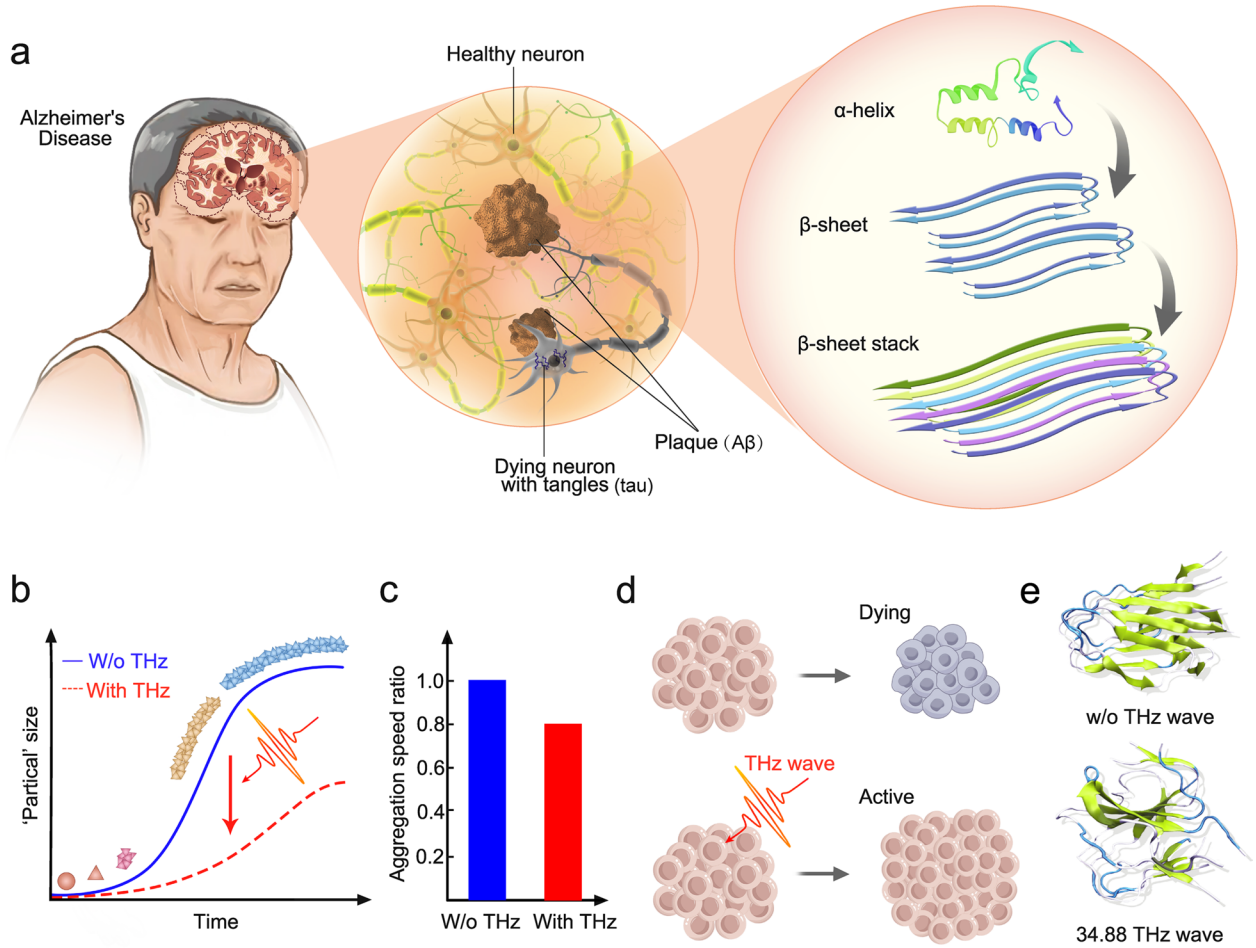

Fig. 1 Schematic of the main content of this study. **a** The presence of extracellular β-amyloid deposition as neuritic plaques and the intracellular accumulation of hyperphosphorylated tau as neuro fibrillary tangles remain the primary neuropathologic features for AD diagnosis, and the amyloid deposition begins with the conversion of native monomers with more α-helices to an alternative conformation with β-sheet that self-associate into ordered assemblies. **b** A terahertz (THz) wave at a frequency of 34.88 THz delays the fibrosis dynamic curve. **c** The wave decreased the aggregation speed to 80% of the case without the wave. **d** The wave promotes cell proliferation. **e** The wave loosens the dense protein conformation with transformed β-sheets to a structure with more coil and bend regions

In 2018, Liu [13] conjectured that the physical field of biological neural signals might be a high-frequency electromagnetic field ranging from terahertz (THz, 10^{12} Hz) to infrared, most likely from 0.5 to 100 THz and named it a generalized terahertz electromagnetic (THz EM) wave. Moreover, some physiological processes have been proven to be regulated by THz fields, such as the unwinding of DNA hairpins [14], the permeability of the voltage-gated calcium channel [15] and the currents of voltage-gated K^+ [16]. The mechanism is that the THz wave resonates with the molecular population and modifies the hydrogen bonds (H-bonds) formed therein. Moreover, it was reported that the intermolecular H-bond network parallel to the fibril axis is the key to guiding the development of amyloid fibrils [17]. Inspired by these findings, it would be valuable in the prevention or mitigation of AD pathology if resonant features could be exploited to modulate the self-assembly process and prevent undesired protein aggregation. Indeed, Kawasaki et al. found that a 1675 cm^{-1} (50.25 THz) light could dissociate amyloid fibrils by a joint method of molecular dynamics (MD) simulation and free electron laser experiment [7]. However, a significant thermal effect occurred at this frequency, because biological liquid has a strong absorption in the range of 45–52.5 THz (Fig. 2b), considerably weakening the regulatory efficiency in the physiological environment. Therefore, there is an urgent need to explore efficient nonthermal methods to inhibit the Aβ aggregation process.

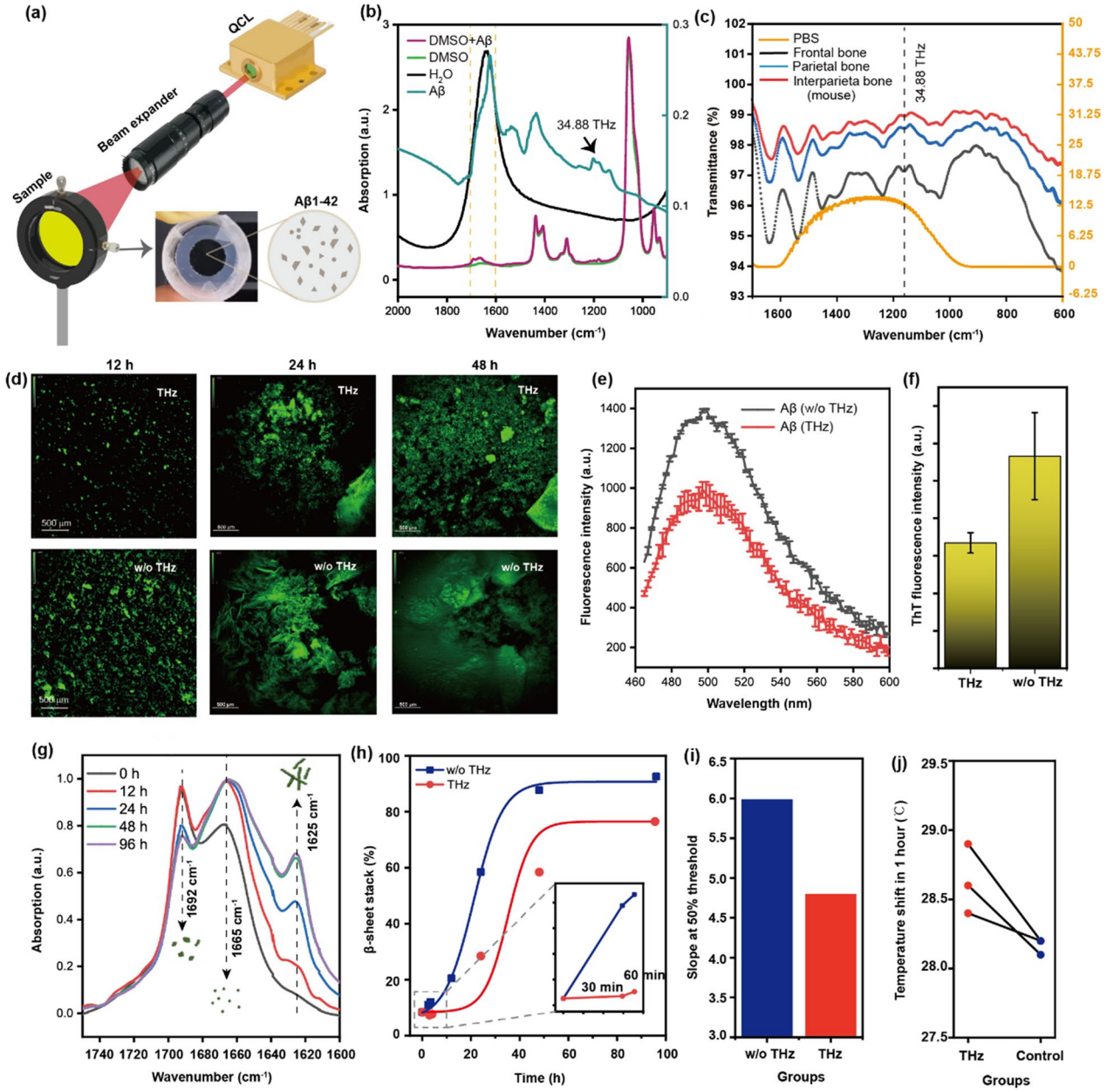

Fig. 2 Fluorescence and spectroscopy experiments show 34.88 THz wave delays the aggregation of Aβ1–42 oligomers. **a** Schematic of the THz optical path system on Aβ1–42 oligomers. **b** The absorption spectra of DMSO, H_2O, DMSO + Aβ and Aβ powder in the range from 900 to 2000 cm^{-1}. **c** Transmission spectra of mouse skull and phosphate buffer solution (PBS). **d** Thioflavine T (ThT) fluorescent images in 48 h of Aβ1–42 fibrosis progression in cases without and with 34.88 THz-wave, respectively. **e**–**f** The fluorescence spectra (**e**) and the intensity (**f**) of ThT in 48 h. **g**–**h** The changes in amide I in 96 h and the percentage composition of the β-sheet stack (reflected by the ratio of the peak areas at 1625 cm^{-1} to those at 1692 cm^{-1} and 1665 cm^{-1}) of Aβ1–42 oligomers in absence of the THz wave (**g**), and the fibrosis kinetic curves fitted through the Boltzmann function (**h**). **i** The slope at 50% threshold value of the curves with and without THz waves. **j** The temperature shifts in 1 h with THz-wave irradiation that is monitored by the liquid probe

In this work, we use a quantum cascade laser (QCL) with a center frequency of 34.88 THz (8.6 μm) to irradiate the Aβ1–42 oligomers, monitored the fibrosis process by thioflavine T (ThT) binding assay and Fourier transform infrared (FTIR) spectrometer and we found that the fibrosis process was significantly slowed down (Fig. 1b, c) compared to the group without an external-field. Additionally, the safety of this frequency at the cell level was also detected through cell viability (Fig. 1d) and mitochondrial membrane potential assays. The cells

proliferated significantly, and there was a slight increase in mitochondrial membrane potential, which demonstrated that THz waves may have a positive effect on cell function. Moreover, the MD simulation result shows a significant change in protein conformation from a regularly ordered structure to a disordered structure (Fig. 1e), specifically, with the transformation of β-sheet structure transformed to coil and bend regions. In summary, THz waves may be a promising strategy to delay the amyloid fibrillation process.

2 Results and discussion

The approach to assessing the oligomeric behavior of Aβ1–42 by 34.88 THz EM wave is shown in Fig. 2a. Through the beam expander the spot size was enlarged to equal the same as the inner diameter of the silicone gasket of the liquid cell. Here, we use DMSO to solvate the oligomer. Figure 2b shows the spectra of H_2O, DMSO and DMSO + Aβ and Aβ powder, revealing that DMSO exhibits low absorption at a frequency of 34.88 THz and wavenumber range of 1600–1700 cm^{-1} (this range was used to characterize the changes in protein secondary structure) compared to water. Moreover, from the mixed spectrum of DMSO plus Aβ and Aβ powder, we can see a slight absorption peak specifically for Aβ (black arrow), which demonstrated the ability to achieve a high-efficiency absorption for the protein. Figure 2c shows the transmission spectra of the mouse skull and phosphate buffer solution (PBS). A relatively high transmittance was observed at the band of 34.88 THz, indicating great potential for the experiment in an AD animal model. Then, a standard ThT fluorescence binding assay was employed to detect the process of aggregation [5]. The fluorescence images of the fibrotic process at 48 h without and with the THz wave are shown in Fig. 2d. In the control group, the fluorescence signal became stronger than that in the THz group at 12 h, followed by the formation of silk-like structures in the next 12 h, which eventually grew into a thick plaque. In contrast, the protein in the THz group still exhibited granulated conditions, but the detailed structure was unclear, which needs other techniques with higher resolution to detect [18], such as electron microscopy. From the results of Fig. 2e, f, we can see that the fluorescence intensity was also lower than that of the control group. Although THz waves have an impact on fluorescence, we noticed that THz waves may enhance the fluorescence emission [19, 20], rather than restrain the emission of fluorescence. Therefore, the observed decrease in fluorescence intensity can be attributed to the fact that the THz wave transformed the protein to another structure with less β-sheet structure. The fibrotic process was also monitored by means of Fourier transform infrared (FTIR), since the amide I band is sensitive to protein secondary structure [21], so FTIR spectroscopy is usually used to diagnose the process of protein misfolding and aggregation in vitro [22, 23]. The major difficulty with measuring the FTIR spectra of proteins is the strong water bending mode that overlaps the amide I vibration characteristics. Some studies have used the D_2O for the protein solution, where the O-D bending mode is shifted to a lower frequency, but we found the low solubility when injecting the Aβ1–42 powder into D_2O, so the solvent was replaced with DMSO. The spectrum of DMSO has been mentioned above, and the weak peak there was easy to be subtracted from the spectrum that mix with the Aβ 42 peptide. Figure 2g shows the absorption spectra (amide I) of the progressive peptide that was collected in 96 h. As previously reported [24], 1692 cm^{-1} and 1695 cm^{-1} are attributed to the oligomers. The vibration absorption of α-helix occurs at 1665 cm^{-1} which mainly exists in monomers and the peak at 1625 cm^{-1} or 1630 cm^{-1} is attributed to the β-sheet in fibrils. The area under the corresponding absorption peak was calculated to estimate the relative content of each secondary structure [21]. Figure 2h shows that the percentage content of β-sheet stacks (1625 cm^{-1}) exponentially accumulated within 48 h, accompanied by a decrease in oligomers (1692 cm^{-1}) and monomers (1665 cm^{-1}). After 48 h, the progression of fibrosis gradually slows and eventually equilibrates with the monomer. Here, we fitted the progress with the Boltzmann function and found that the improvement rate slowed markedly after THz irradiation in the early phase, especially in the first hour. The slope at 50% of the threshold value is shown in Fig. 2i. The aggregation speed ratio decreased to approximately 80% when the THz wave was loaded. In all of the tests based on the Aβ oligomer, we saw that the THz wave at 34.88 THz could significantly slow down the fibrotic progression.

There is no doubt that the thermal effect is a very important factor should to be considered, whether the proteins are thermally denatured or not during the process. Thus, we measured the temperature change by using various tools including liquid probes, solid contact probes and forward-looking infrared (FLIR). When the parameters of the QCL were set at a repetition rate of 100 kHz with a 2 ms pulse width, the current was carried out at 1050 mA with an 8% duty ratio, we observed that the temperature shifted no more than 0.5 °C in 1 h (Fig. 2j). Delport et al. reported that the average melting temperature for amyloid precursor protein is 55.9 °C [25], so we concluded that no denaturation occured. To determine whether the dissociation efficiency increases with increasing temperature below the denaturation temperature, we set up another experiment that placed the oligomers in a 37 °C cell incubator for two hours and

found that the increase in temperature did not inhibit but promoted fibrosis (Additional file 1: Note 2), which is consistent with the results from other published reports [26]. Specifically, Kusumoto et al. demonstrated that the elongation rate of Aβ fibrils varies over two orders of magnitude within the temperature range of 4–40 °C and obeys the Arrhenius law [26]. Actually, we have performed much work on THz waves [27–30] and have a deep understanding of the properties. There is a non-linear relationship between the power and the efficiency of protein dissociation [31, 32]. For example, water permeation across a water channel could be strongly and nonlinearly modulated by the electric-component strength of a 1.39 THz-EM wave, but is weakly and linearly affected by temperature. The phenomenon also exhibits a frequency-dependent behavior.

To investigate whether THz waves have a protective effect against oligomeric toxicity, and the effect of the wave on the function of the cell itself, we designed some experiments based at the cellular level. Figure 3a shows the schematic of the scheme. There were four groups, with and without oligomers and with and without THz waves. In fact, during irradiation, we designed a special petri dish with a CaF_2 bottom for a high transmittance of the field to the adherent cell, see Additional file 1: Note 3 for details. Figure 3b shows the time and frequency of the radiation. Figure 3c, d shows the corresponding results. It can be seen that the fluorescence intensity in the THz group is also lower than that in the control group, which is consistent with the result of oligomers. With regard to cell viability, it was found that most of the cells floated in the groups with oligomers-added, so the cell viability could not be detected, but the cells grew well in the control and THz-irradiation groups. Cells viability was detected by a cell counting kit (CCK-8). We can see that the absorption increased significantly ($p < 0.01$) in the THz-loaded group (Fig. 3e). Moreover, we used Hoechst 33342 dye to visualize the cell proliferation, it can be seen that the number of the cells was greater than that in the control group (Fig. 3g). Additionally, we also used mitochondrial membrane potential (MMP) as another index to reflect the function of cells. The results are shown in Fig. 3h. Although there was no significant difference between the groups, the group exposed to THz waves showed a slight increase. The detailed information was shown in supporting information (Additional file 1: Note 3 and Figure S7). These results demonstrate that THz waves are at least somewhat safe according to the cell

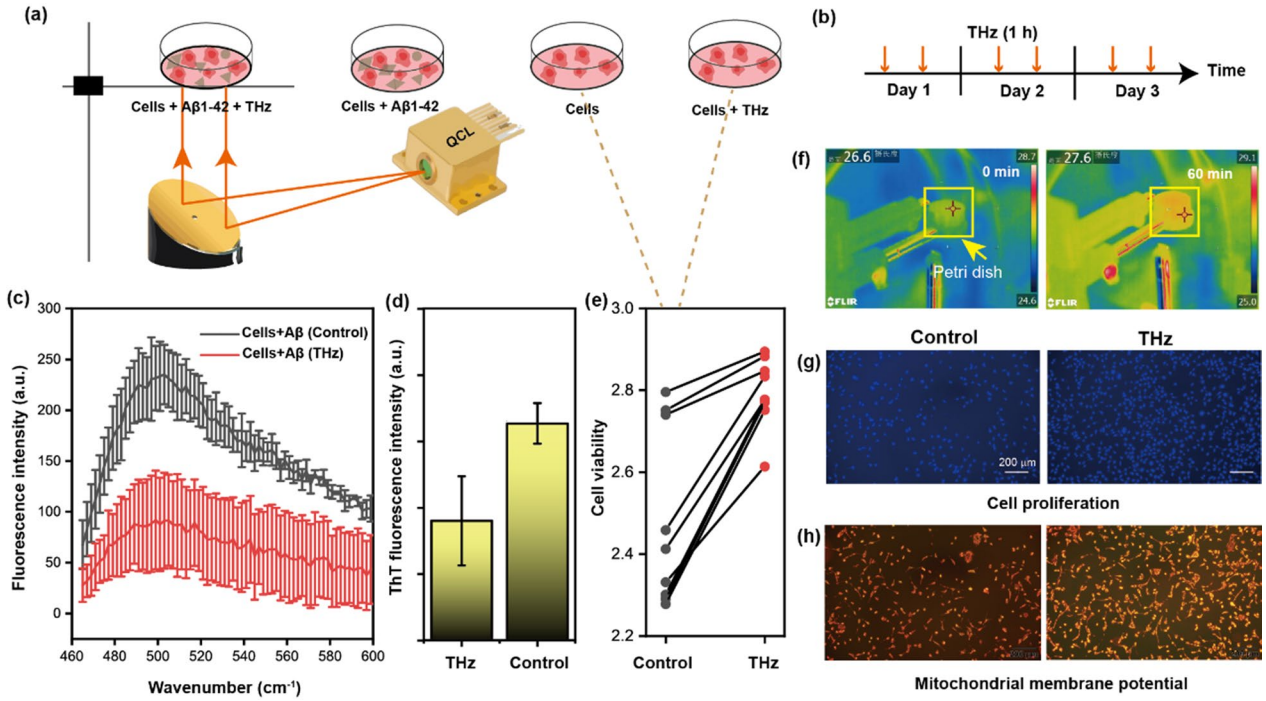

Fig. 3 Cell experiments show that the 34.88 THz wave dissociates oligomers and promotes cell proliferation. **a** Schematic diagram of loading oligomers and terahertz waves on cultured cells. **b** The time and frequency of the loading terahertz wave. **c**–**d** The fluorescence spectra (**c**) and intensity (**d**) of ThT. **e** Cell viability before and after THz irradiation. **f** The temperature shift over 1 h with THz-wave irradiation that is monitored by forward-looking infrared (FLIR). **g** The cells were stained with Hoechst 33342 to reflect cell proliferation. **h** The level of mitochondrial membrane potential in the control and THz groups

performance. Figure 3f shows the temperature change during the radiation. Actually, the bioeffects of THz-wave exposure have been reported in many studies. Zhao et al. [33] demonstrated that a single-frequency THz laser increases excitatory synaptic transmission and neuronal firing activities when conducted on cultured mice cortical neurons. Zhang et al. [34] reported that THz waves at 53.57 THz could activate brain neurons in vivo without introducing any exogenous gene, and during an auditory associative task, the mice that received THz waves targeting the auditory cortex exhibited faster learning speed than the control mice. Moreover, Abufadda et al. [35] found that THz pulses could stimulate cell proliferation and both histogenesis and organogenesis, producing a significantly higher number of regenerated segments of earthworms. All of the above reports indicate positive excitation by THz irradiation, so it can be considered that THz waves may play a dual role in the neuronal activity and instability of the Aβ fibril.

It is complicated to explain the effect, because the band at 34.88 THz is attributed to the vibration of C–O (H) stretching in proteins [36] and the mechanism for the delay unclear. Thus, we developed a system that contains the Aβ1–42 oligomer and water with 0.15 M NaCl, the cartoon diagram is shown in Fig. 4. Through a long-time MD simulation and the trajectory of all atoms in the system was analyzed by the interface of do_dssp of GROMACS software, it was found that the number of residues exhibiting each type of secondary structure with and without the THz wave showed a significant difference, especially in the coil, β-strand and bend regions (Fig. 4c). Specifically, THz waves transform the structure of β-sheets to more coil and bend content and thus loosen the dense fibril structure. Moreover, we also take a test on the fibril obtained from cryo-electron microscopy (PDB: 5OQV) and counted the percentage change in β-strands, it also can be seen a significant decrease in the structure. The detailed information

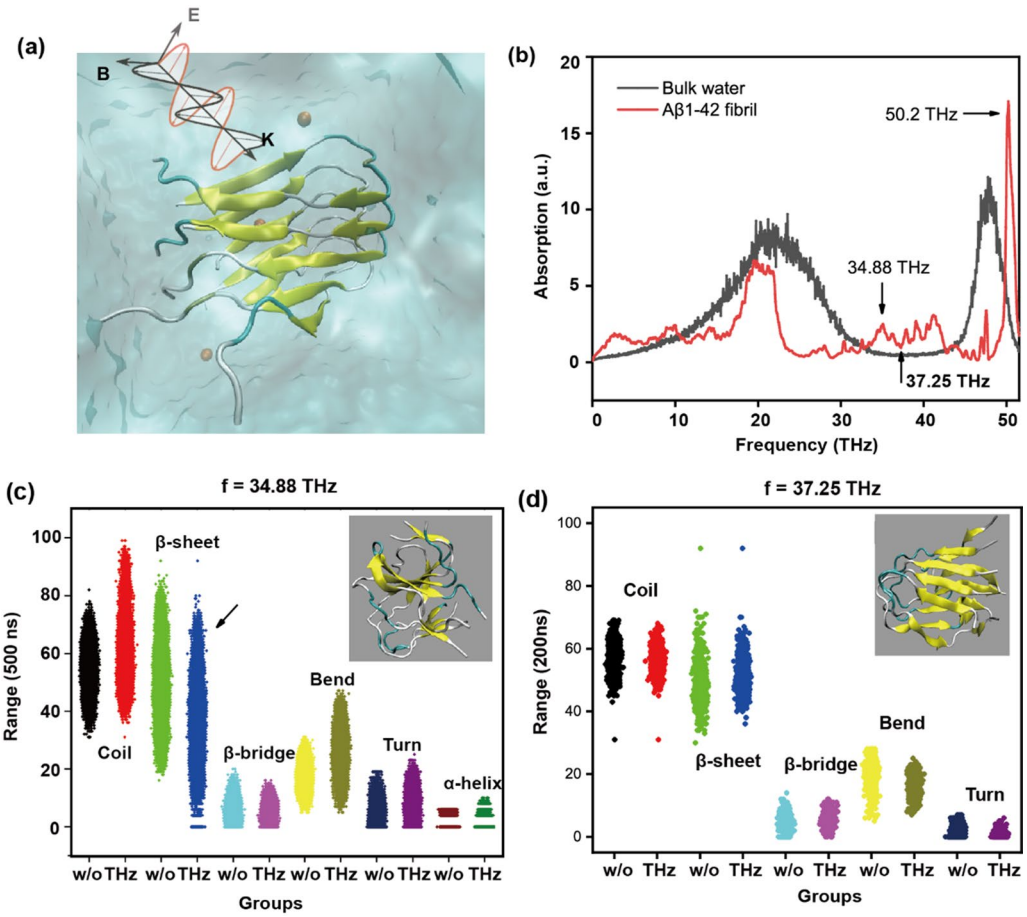

Fig. 4 Terahertz waves loosen the fibril conformation by transforming the β-sheet structure to contain more coil and bend regions. **a** Schematic of the Aβ1–42 simulation system in 0.15 M NaCl in water. **b** The THz spectrum of bulk water and Aβ1–42 fibrils in the range from 0 to 50 THz. **c** Changes in the secondary structure of the protein irradiated by a 34.88 THz wave. **d** Changes in the secondary structure of the protein irradiated by a 37.25 THz wave

shown in Additional file 1: Note 4. According to the optimal system and the trajectory file, the THz spectrum of the system was calculated and is shown in Fig. 4b, it can be seen that the Aβ1–42 fibril also has a strong absorption at 34.88 THz while avoiding the water vibration peak, which demonstrated that the protein system could resonate with this specific frequency and provide the dissociation force. Moreover, we analyzed the low absorption frequency of 37.25 THz, and the change of the secondary structure shown in Fig. 4d, and we found no significant difference between the groups with THz weakly absorbed by protein. To strengthen this conclusion, we conducted an experiment using a light frequency that was weakly absorbed by the protein. The result still shows that the light did not reduce the rate of fibrosis (Additional file 1: Note 4 and Figure S9), which further demonstrates that the effect of light on the fibril formation process shows a frequency-dependent characteristic. In fact, numerous researchers use micromolecules to destabilize the fibrils, which also means to intervene the secondary structure. For example, Kanchi et al. [37] concluded that proline could be considered a novel drug to treat AD for the reason that it could break the β-sheet structure and in some cases even induce the formation of 3_{10} helices. Zou et al. [38] reported that norepinephrine molecules could considerably reduce the interpeptide β-sheet content and suppress the formation of β-hairpin, leading to a more disordered coil-abundant Aβ dimer, and thus could be considered as a therapeutic strategy for AD. Most of the studies remain at the theoretical stage and lack experimental verification. In this study, we developed an effective method that is mainly based on non-thermo-optical modulation, and also proved its effectiveness in experiments. Thus, we conclude that the THz wave at the specific band of 34.88 THz could serve as a novel pattern to destabilize fibrils.

3 Conclusion

In this study, we developed a novel dissociation mode with THz waves that delays the kinetic progression of amyloid fibrils. The mechanism was not based on protein degeneration but changed the conformation by transforming the structure of β-sheets to a looser structure with more coil and bend regions. The results were also verified by ThT fluorescence and spectroscopy of the protein secondary structure. Additionally, the results indicated the safety of this frequency at the cellular level through cell viability and MMP assays. Although we did not observe an obvious protective effect on cell function when surrounded by toxic oligomers, we still detected a reduction in the fluorescence intensity of ThT, which indicates a decrease in the content of the β-sheet structure. This discovery has important implications for the prospects of a wide range of applications, for example, as an adjunct to the treatment of AD or other amyloid-related pathologies.

4 Materials and methods

4.1 Sample Preparation

The Aβ1–42 peptide was purchased from Bioss (Cat. No. bs-0107P). Dimethyl sulfoxide (DMSO) was purchased from Beyotime (Cat. No. ST038). The rubber gaskets and CaF_2 windows were purchased from TianGuang (FHGCP) with sizes of 0.5 mm thickness and 25 mm diameter * 2 mm thickness, respectively. Hexafluoroisopropanol (HFIP) was purchased from Macklin (Cat. No. H811027) and thioflavine T (ThT) dye were purchased from Keygen Biotech Company (Cat. No. KGMP0241).

4.2 Parameters of the Quantum Cascade laser (QCL)

The QCL was provided by the Institute of semiconductors of Chinese Academy of Sciences. The center frequency of the QCL is 34.88 THz, with a bandwidth that extends below 35.4 THz and above 34.6 THz. During the irradiation, the repetition rate was set to 100 kHz with a 2 ms pulse width, the current was carried out at 1050 mA with an 8% duty ratio, and the power of the light outlet was 15 mW and decreased to 14.25 mW when passing through the window of CaF_2 material with a power density of 0.73 mW/mm^2. The detailed information is presented in Additional file 1: Note 1.

4.3 Preparation of Aβ1–42 Oligomer

First, the Aβ1–42 peptide powder was dissolved in cooling HFIP, and then incubated at room temperature for 60 min. Afterward, the mixture of peptide-HFIP was placed on ice for 5–10 min and moved to a fume cupboard to allow HFIP to evaporate. After air drying, the transparent Aβ peptide membrane was dissolved in fresh 100% DMSO (5 mM synthesized peptide).

4.4 Protein experiment

A silicone gasket with a thickness of 0.5 mm, outer diameter of 18 mm and inner diameter of 10 mm was placed between two calcium fluoride windows (sandwich-like). The power of the light outset was 11.5 mW, and after the beam expander the spot diameter was expanded to ~5 mm. Fifty μl of 5 mM Aβ peptides (residues 1–42) was injected into the groove and sealed with parafilm around the window. The experimental group was treated with THz waves and the ThT dye was used to monitor the content of the β-sheet structure. Fluorescence intensity was detected by a multimode reader (Thermo Fisher) and the fluorescent images were collected by fluorescence microscopy. The spectra collected by FTIR and the content of the secondary structure were characterized

through amide I deconvolution by using PeakFit v4.12 software.

4.5 Cell experiment

The oligomer was diluted in 1640 medium to a final concentration of 50 nM and was used to culture the SH_SY5Y cells. During the process, we exposed the cells to the THz field (the power density was the same as the protein experiment with 0.73 mW/mm^2) twice a day, and the duration time was 1 hour for a single administration. Three days later, we detected the fluorescence intensity of the ThT dye. The control group was not administered radition, but the other experimental conditions were consistent with those in the THz group. The cell viability and MMP assays were detected 4 hours later after THz radiation, and the test products were purchased from Beyotime (C0037, C2006) and ThermoFisher (Hoechst 33342).

4.6 Molecular dynamics stimulation

In this research, all molecular dynamics simulations with and without the THz-EM waves were carried out at the temperature of 310.15 K using GROMACS software. Each simulation consists of four processes with different ensembles including energy minimization, NVT/NPT equilibrium, and production simulation. The step of energy minimization was initially used to obtain a reasonable conformation system, then the NVT and NPT ensembles were used to make the system to the expected temperature and reasonable density under a pressure of approximately 1.0 bar. Finally, the production simulation was applied to collect the trajectory of the conformations in the equilibrium process for the analysis. During the simulation, the equation of motion was solved by the Velocity-Verlet integrator with a time step of 2 fs under periodic boundary conditions, and the force field parameters of all the molecules were characterized by the gromos54a7 force field. Furthermore, the electrostatic interactions were treated using the particle mesh Ewald algorithm and all bond lengths were constrained by the LINCS algorithm.

Supplementary Information

The online version contains supplementary material available at https://doi.org/10.1186/s43593-023-00048-0.

Additional file 1: Notes 1–4.

Acknowledgements

This work was supported by Innovation Laboratory of Terahertz Biophysics and financially supported by the National Natural Science Foundation of China (Grants No. 12225511, T2241002) and the key innovative project in Shaanxi (No. 2021ZDLSF02-02, 2022KXJ-123), and sponsored by Shanghai Rising-Star Program (No. 23QA1404200). We also thank the computing resources and technical support from Shanghai Snowlake Technology Co. Ltd.

Author contributions

WYP, ZZ, YMW and CC conceived the idea, YMW and CC supervised the project. WYP and ZZ designed and performed the experiments. WYP, ZZ and KC analyzed the data, WYP, ZZ and CC drafted the paper with input from all authors. All authors read and approved the final maunscript.

Declarations

Competing interests

The authors declare no competing interest.

Received: 26 February 2023 Revised: 2 April 2023 Accepted: 14 May 2023
Published online: 01 August 2023

References

1. P.H. Nguyen, B.R. Ramamoorthya sahoo et al., Amyloid oligomers: a joint experimental/computational perspective on Alzheimer's disease, Parkinson's disease, type II diabetes, and amyotrophic lateral sclerosis. Chem. Rev. **121**(4), 2545–2647 (2021)
2. M.I. Vaquer-alicea, J. Diamond, Propagation of protein aggregation in neurodegenerative diseases. Annu. Rev. Biochem. **88**, 785–810 (2019)
3. G. Meisl, S. Michaels, T.C.T. Linse et al., Kinetic analysis of amyloid formation. methods. Mol. Biol. **1779**, 181–96 (2018)
4. J.A. Sawaya, M.R. Hughes, M.P. Rodriguez et al., The expanding amyloid family: structure, stability, function, and pathogenesis. Cell **184**(19), 4857–4873 (2021)
5. S. Head, C.C. Hsu, T.M. Bi et al., Alpha-sheet secondary structure in amyloid beta-peptide drives aggregation and toxicity in Alzheimer's disease. Proc. Natl. Acad Sci. USA **116**(18), 8895–900 (2019)
6. S. Jokar, S. Khazaei, H. Behnammanesh et al., Recent advances in the design and applications of amyloid-beta peptide aggregation inhibitors for Alzheimer's disease therapy. Biophys. Rev. **11**, 901–925 (2019)
7. T. Kawasaki, Y. Man, V. H. Sugimoto et al., Infrared laser-induced amyloid fibril dissociation: a joint experimental/theoretical study on the GNNQQNY peptide. J. Phys. Chem. B **124**(29), 6266–6277 (2020)
8. E.N. Wilson, K.I. Andreasson, TAM-ping down amyloid in Alzheimer's disease. Nat. Immunol. **22**(5), 543–544 (2021)
9. J.M. Long, D.M. Holtman, Alzheimer disease: an update on pathobiology and treatment strategies. Cell **179**(2), 312–339 (2019)
10. T.M.A. Busche, B. Hyman, Synergy between amyloid-beta and tau in Alzheimer's disease. Nat. Neurosci. **23**(10), 1183–1193 (2020)
11. P. Saha, S.E.N.N. Tauopathy, A common mechanism for neurodegeneration and brain aging. Mech. Ageing Dev. **178**, 72–79 (2019)
12. S. Brahmachari, A. Paul, D. Segal et al., Inhibition of amyloid oligomerization into different supramolecular architectures by small molecules: mechanistic insights and design rules. Future Med. Chem. **9**(8), 797–810 (2017)
13. LIU G, The conjectures on physical mechanism of vertebrate nervous system. Chin. Sci. Bull. **63**(36), 3864–3865 (2018)
14. K. Wu, C. Qi, Z. Zhu et al., Terahertz wave accelerates DNA unwinding: a molecular dynamics simulation study. J. Phys. Chem. Lett. **11**(17), 7002–7008 (2020)
15. Y. Li, C. Chang, Z. Zhu et al., Terahertz Wave enhances permeability of the voltage-gated calcium channel. J. Am. Chem. Soc. **143**(11), 4311–4318 (2021)
16. X. Liu, Z. Qiao, Y. Chai et al., Nonthermal and reversible control of neuronal signaling and behavior by midinfrared stimulation. Proc. Natl. Acad. Sci. USA **118**(10), 2015685118 (2021)
17. C.M. Vendruscolom Dobson, T.P.J. Knowles, The amyloid phenomenon and its significance in biology and medicine. Cold Spring Harbor Perspect. Biol. **12**(2), a033878 (2020)
18. J. Qian, Y. Cao, Y. Bi et al., Structured illumination microscopy based on principal component analysis. eLight. **3**(1), 4 (2023)

19. J. Liu, X.C. Zhang, Terahertz-radiation-enhanced emission of fluorescence from gas plasma. Phys. Rev. Lett. **103**(23), 235002 (2009)
20. J. Liu, J. Dai, S.L. Chin, X.C. Zhang, Broadband terahertz wave remote sensing using coherent manipulation of fluorescence from asymmetrically ionized gases. Nat. Photonics **4**(9), 627–631 (2010)
21. F.S. Ruggeri, G. Longo, S. Faggiano et al., Infrared nanospectroscopy characterization of oligomeric and fibrillar aggregates during amyloid formation. Nat. Commun. **6**, 7831 (2015)
22. L. M. Miller, M. W. Bourassa, R. J. Smith, FTIR spectroscopic imaging of protein aggregation in living cells. Biochim. Biophys. Acta **1828**(10), 2339–2346 (2013)
23. T. Moran, S.D. Zanni, How to get insight into amyloid structure and formation from Infrared spectroscopy. J. Phys. Chem. Lett. **5**(11), 1984–1993 (2014)
24. R. Sarroukh, J.M. Goormaghtgh, E. Ruysschaert et al., ATR-FTIR: a "rejuvenated" tool to investigate amyloid proteins. Biochim. Biophys. Acta **1828**(10), 2328–2338 (2013)
25. A. Delport, Determining the protein stability of Alzheimer's disease protein, amyloid precursor protein. Protein J. **38**(4), 419–424 (2019)
26. Y. Kusumoto, A. Lomakin, D.B. Teplow et al., Temperature dependence of amyloid beta-protein fibrillization. Proc. Natl. Acad. Sci. USA **95**(21), 12277–12282 (1998)
27. J. Lou, Y. Jiao, R. Yang et al., Calibration-free, high-precision, and robust-terahertz ultrafast metasurfaces for monitoring gastric cancers. Proc. Natl. Acad. Sci. USA **119**(43), e2209218119 (2022)
28. W. Peng, S. Chen, D. Kong et al., Grade classification of human glioma using a convolutional neural network based on mid-infrared spectroscopy mapping. J. Biophotonics (2022).
29. W. Peng, S. Chen, D. Kong et al., Grade diagnosis of human glioma using Fourier transform infrared microscopy and artificial neural network. Spectrochim. Acta, Part A **260**, 119946 (2021)
30. W. Peng, J. Yin, J. Ma et al., Identification of hepatocellular carcinoma and paracancerous tissue based on the peak area in FTIR microspectroscopy. Anal. Methods. **14**(32), 3115–3124 (2022)
31. Z. Zhu, C. Chang, Y. Shu et al., Transition to a superpermeation phase of confined water induced by a terahertz electromagnetic wave. J. Phys. Chem. Lett. **11**(1), 256–262 (2019)
32. T. Sun, Z. Zhu, Light resonantly enhances the permeability of functionalized membranes. J. Membr. Sci. **662**, 121026 (2022)
33. X. Zhao, M. Zhang, Y. Liu et al., Terahertz exposure enhances neuronal synaptic transmission and oligodendrocyte differentiation in vitro. iScience **24**(12), 103485 (2021)
34. J. Zhang, Y. He, S. Liang et al., Non-invasive, opsin-free mid-infrared modulation activates cortical neurons and accelerates associative learning. Nat. Commun. **12**(1), 2730 (2021)
35. M.H. Abufadda, A. Erdelyi, E. Pollak et al., Terahertz pulses induce segment renewal via cell proliferation and differentiation overriding the endogenous regeneration program of the earthworm Eisenia andrei. Biomed. Opt. Express **12**(4), 1947–1961 (2021)
36. X. Wang, X. Shen, FTIR spectroscopic comparison of serum from lung cancer patients and healthy persons. Spectrochim. Acta. Part A **122**, 193–197 (2014)
37. A.K. Kanchi, P.K. Dasamahapatra, Polyproline chains destabilize the Alzheimer's amyloid-beta protofibrils: a molecular dynamics simulation study. J. Mol. Graph Model **93**, 107456 (2019)
38. Y. Zou, Z. Qian, Y. Chen et al., Norepinephrine inhibits Alzheimer's amyloid-beta peptide aggregation and destabilizes amyloid-beta protofibrils: a molecular dynamics simulation study. ACS Chem. Neurosci. **10**(3), 1585–1594 (2019)